Attachment A

2020 Ozone Exceptional Events Analysis for the District of Columbia

Introduction

Tropospheric ozone (O_3) is a major component of photochemical smog. This reactive molecule is known to have harmful effects on human health, vegetation, visibility, and climate (Sousa et al 2008, WHO, EEA). Because it is so unstable and highly reactive, O_3 can readily deposit itself on biological tissues and contributes to premature deaths and other negative health outcomes such as asthma exacerbation. O_3 is a secondary gas, which is created by the photochemical reaction between precursor pollutants, volatile organic compounds (VOCs), and nitrogen oxides (NO_x) in the presence of sunlight. Equations 1-4 explain the formation and depletion of ground-level O_3.

$$2NO + O_2 \rightarrow 2NO_2 \quad (1)$$

$$NO_2 + sunlight \rightarrow NO + O \quad (2)$$

$$O + O_2 \rightarrow O_3 \quad (3)$$

$$O_3 + NO \rightarrow NO_2 + O_2 \quad (4)$$

Firstly, nitric oxide (NO) reacts with oxygen (O_2) to produce nitrogen dioxide (NO_2). In the presence of sunlight, NO_2 breaks apart to form NO and a free oxygen atom. The free oxygen atom collides with molecules of oxygen to form O_3. O_3 is later destroyed by NO to form NO_2 and O_2.

Generally, highest levels of O_3 occur during the hottest part of the year. In the District, the highest O_3 levels are generally seen from May 1st to September 30th. During the day, O_3

typically peaks in the mid to late afternoon when the presence of consistent sunlight helps fuel the reaction.

An increase in the vehicular traffic and industry has caused a rise in this criteria pollutant in urban areas. Levels of O_3 are also known to be influenced by meteorological variables such as temperature, solar radiation, wind speed (upper atmosphere and boundary layer), and relative humidity.[1] Several studies have shown the strong relationship between temperature and surface O_3.[2–4] Camalier et al. 2007 found that temperature was a major driver behind O_3 levels in the northeast,[5] while relative humidity strongly influenced O_3 levels in the southeastern region of the United States.[6] Stratospheric O_3 exchange,[7] along with regional O_3 transport affect the locally observed levels of O_3 at the surface. The primary sinks of ground level O_3 include titration through reactions with nitric oxide (NO) and dry deposition.[8]

The Clean Air Act requires the Environmental Protection Agency (EPA) to set National Ambient Air Quality Standards (NAAQS) for the six criteria pollutants. In 2015, the EPA strengthened the 8-hour NAAQS for O_3 to 70 ppb and in 2018, the District and the surrounding metropolitan area were designated as marginal nonattainment for the 2015 O_3 NAAQS. O_3 in the District is primarily driven from regions upwind of the city. According to modeling performed, and extensive research, nearly 90% of ozone pollution in the DC-MD-VA region is transported from other states.[9,10] However, the 2020 COVID health emergency led to lower O_3 levels in the District due to traffic disruption. Similar phenomena were seen across the country as demonstrated in Chen et al. 2020.[11] During the first half of 2020, global emissions of CO_2 decreased by 8.8% and the European Union reported upwards of 60% reduction for NO_x.[12–14] Goldberg et al. 2020 reported a median drop of 21.6% of NO_2 in 20 North American cities during the spring of 2020.[15] The reductions led to better air quality, but the changes in emissions

are not permanent, nor enforceable. A report from the mobility data firm INRIX stated the DC region had the largest drop in traffic congestion (77%) in 2020 out of other major cities from around the world.[16] The Department of Energy and Environment (DOEE) is petitioning for the 2020 health emergency to be considered an exceptional event. Although exceptional events usually involve exceedances, the 2020 health emergency should also be considered one because it was uncontrollable, caused a decrease in traffic that is not likely to reoccur, and it was directly related to the spread of Covid-19, which evidence points towards being a natural (zoonotic transfer) event, and treating the data as policy relevant can have long term impacts on the air quality of residents of the District of Columbia.

The objective of this study is to build an ozone forecasting tool using meteorological variables from 2013-2017 using quantile regression (QR) and ordinary least squares (OLS) regression. This forecasting tool will then be used to predict ozone for years 2018 and 2019 to demonstrate that the tool produces reasonable results during a typical ozone season and will also be used to predict ozone for 2020, to demonstrate that the 2020 ozone season was atypical despite meteorological factors.

QR is a useful mathematical tool that models the relationship between covariates and quantile functions.[17] This regression is particularly important for environmental studies when explaining outliers and looking at an entire distribution. On the other hand, OLS is a simple model that is used to estimate a relationship between two variables using linear regression. This work will compare the O_3 forecasting results from QR and OLS using meteorological data measured at the McMillan monitoring site in the District.

Methods

The District maintains a network of monitoring stations that measure outdoor air quality. Meteorological variables and concentrations of ozone in this study were recorded at the McMillan Reservoir site (ID:11-001-0043, 38.9218^{o}N, -77.0132^{o}E). The data is integrated into the Air Quality Monitoring Network of the DOEE. Use of monitored data from the Takoma Recreation Center (ID:11-001-0050) and River Terrace (ID:11-001-0041) sites were also considered, but data sets were not complete for the time period examined so they were not used. The meteorological variables and O_3 concentrations were continuously monitored and hourly averages were recorded. O_3 concentrations were measured using UV-absorption photometry. Meteorological variables considered for this study include temperature, pressure, wind speed, wind speed at both 500 and 850 mb, wind direction, wind direction at both 500 and 850 mb, precipitation the day before, relative humidity, global horizontal irradiance and geopotential height. All instruments underwent a rigorous maintenance procedure with periodic calibrations.

Table 1: Instrumentation used in this study. All instruments are located at the McMillan site in the District.

Instrument	**Measurement**
Thermo 49i	Ozone
WXT536	Weather Sensor: Temperature, Humidity, Pressure, Rainfall, Wind
WMT702	Wind Sensor
HMP155	Humidity and Temperature Probe
PTB110	Barometric Pressure

Upper atmosphere variables were obtained from sounding data at Dulles airport in Sterling, VA.[18] Geopotential height data was acquired from European Centre for Medium-Range Weather Forecasts (ECMRWF) reanalysis version 5 or ERA5.[19] 2013-2017 solar radiation data was retrieved from the National Renewable Energy Laboratory (NREL) while 2018-2020 data came from the District's McMillan monitoring site. All meteorological data missing from the McMillan monitoring site was substituted with meteorological data from the District's Near-Road (ID:11-001-0051) site to provide for a more complete data set. The forecasting tool developed in this study uses O_3 season meteorological data and temporal variables (day of the week, hour of the day, year) from years 2013-2017.

The Models

Ordinary Least Squares (OLS)

OLS is a linear least squares method that models the relationship between one or multiple independent variables (x) and the conditional mean of the dependent variable (y) assuming a constant variance. The dependent variable in this study is the 1-hr ozone concentration. OLS is sensitive to outliers and assumes normality. The following equation explains this simple linear regression model:

$$y_i = \alpha + \beta x_i + \varepsilon_i \quad (5)$$

Where α is the y-intercept, β is the population slope coefficient (by minimizing the error of prediction) and ε_i is the error term. There are 55 regressors or independent variables x_i included in this model.

Quantile Regression (QR)

Quantile Regression is an extension of least square regressions where one can study the relationship amongst variables at different distributions. These different distributions are quantiles (τ or percentiles). This statistical modeling tool was first developed by Koenker and Bassett (1978) and is considered a robust method of analysis to outliers in a dataset.[20] It provides a more comprehensive overview of the independent variable's effect on the dependent variable. The QR model equation for the τth quartile is as follows

$$Q_\tau(y_i) = \beta_0(\tau) + \beta_1(\tau)x_{i1} + \cdots + \beta_p(\tau)x_{ip} \qquad (6)$$

where *p* is the number of regressor variables, $\beta_0(\tau)$ is a constant and $\beta_p(\tau)$ are the coefficients at several quantiles. Further information on QR can be found in Baur et al. 2004.[21] There are also 55 regressors or independent variables x_{ip} included in this model.

Performance Index Parameters

The performance of the QR and OLS models was evaluated by calculating the following statistical parameters: normalized mean bias (NMB), normalized mean error (NME) and root mean square error (RMSE).

NMB averages the difference (model-observations) over the sum of the observed values. It is defined as:

$$NMB = \frac{\sum_1^n (P-O)}{\sum_1^n (O)} \qquad (7)$$

where P is the predicted concentrations and O is the observed concentrations. Similar to NMB, NME looks at the absolute value of the difference over the sum of the observed values. NME is defined as:

$$NME = \frac{\sum_1^n |P-O|}{\sum_1^n (O)} \qquad (8)$$

RMSE is a metric that tells the average distance between the modeled values to the observed values. RMSE is defined as:

$$RMSE = \sqrt{[\sum_{i=1}^{N} (z_{fi} - z_{0i})^2 / N]} \qquad (9)$$

Results and Discussion

The study was performed to predict ozone levels for the District. Several predictor variables were used, and the data was divided into three datasets: (i) 2013-2017; (ii) 2018-2019; and (iii) 2020.

Ozone and Temperature

The relationship between O_3 and temperature in the District was evaluated using linear regression analysis. Previous studies have shown temperature being a good predictor of ground-level O_3. Higher temperatures speed up the rate of chemical kinetics and increase the emissions of biogenic VOCs. Figures 2a-c show the correlation between O_3 and ambient temperature for the McMillan site during the O_3 season. Data from years 2013-2017 were used to create the model. The model was used to predict O_3 levels in 2018 and 2019 and compared to ambient data in those respective years. 2020 was the year of the exceptional event, and the model developed with 2013-2017 data was compared to ambient 2020 data using QR and OLS.

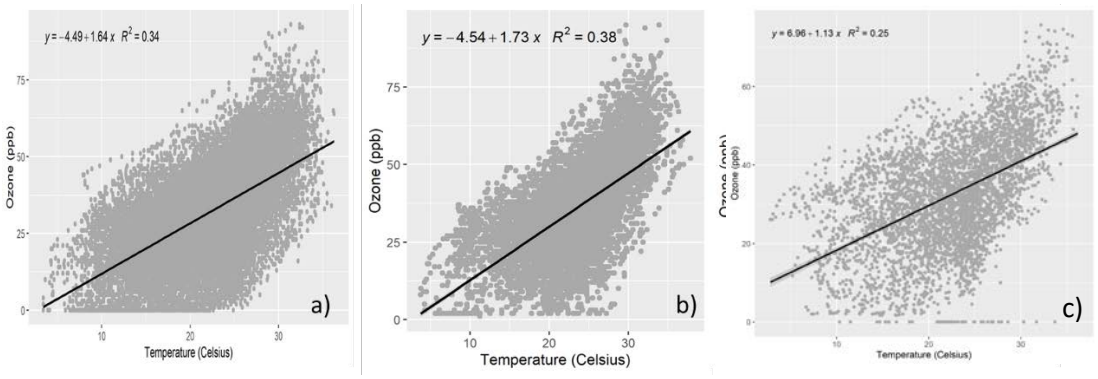

Figure 2: Correlation of O_3 and ambient temperature during years a) 2013-2017 b) 2018-2019 c) 2020.

For all years, O_3 generally increased with temperature. The linear fit for years 2013-2017 (Figure 2a) and 2018-2019 (Figure 2b) yielded very similar slopes. The statistical results are provided in Table 2. It was observed that there was some non-linearity at higher temperatures and QR is a useful tool that accounts for heterogeneity of extreme values.

Ozone and Relative Humidity

Relative humidity is another meteorological variable that influences tropospheric O_3 variation. Simple regression analysis was used to assess the influence of relative humidity on ozone formation. Results from the McMillan monitor indicate an inverse relationship between the two variables. Previous studies have also shown this strong negative correlation.[22–27] Figures 3a-c show this correlation for ozone season during the different groups of years. Table 2 provides the linear regression coefficients.

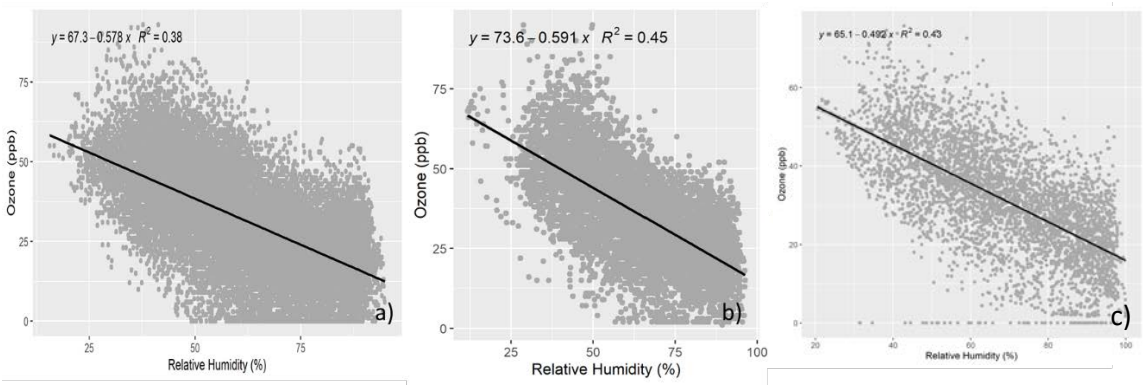

Figure 3: Correlation of O_3 and ambient relative humidity during years a) 2013-2017 b) 2018-2019 c) 2020. The different grouped years have similar slopes.

Some factors to explain this inverse relationship between ozone and relative humidity include the following: (1) humid days associated with increased cloud cover and thus less solar radiation for photochemical reactions, (2) humid days associated with precipitation and the reduction of precursor emissions, (3) stratospheric intrusions of dry, ozone rich air,[27] and (4) affects chain termination reactions.[22]

Ozone and Wind Speed

Regression analysis was used to characterize the relationship between hourly O_3 and hourly wind speed in the District. Dueñas et al. reported that wind speed is one of the most influential meteorological variables to impact ozone concentrations at their coastal site.[22] Wind speed is known to be an important factor for pollution dispersion and for stratospheric ozone transport. Within the District, a weak positive correlation was observed for the several years of analysis. Figures 4a-c depicts this relationship.

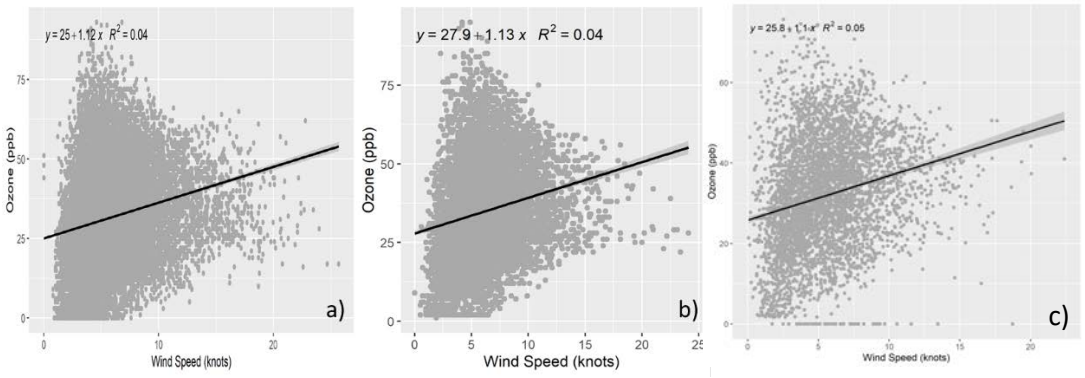

Figure 4: Correlation of O_3 and ambient wind speed during years a) 2013-2017 b) 2018-2019 c) 2020. The different grouped years have weak correlations with similar slopes.

Generally, a rise in wind speed leads to a rise in the transport of air masses, and thus a dilution in primary pollutants. However, this is more complex for secondary pollutants such as ozone. Higher wind speeds induce lower NO_x, and subsequently higher O_3.[28–30] Northern cities on the east coast are more influenced by transport and cities downwind major sources may encounter an increase in O_3 at higher wind speeds.[31]

Ozone and Global Horizontal Irradiance (GHI)

GHI is a measurement of the total irradiance from the sun on a horizontal surface. In the District, O_3 saw a positive correlation with solar radiation. An increase in solar irradiance leads to an increase in photochemical reactions that induce O_3 formation. Figures 5a-c show the correlation between the two variables.

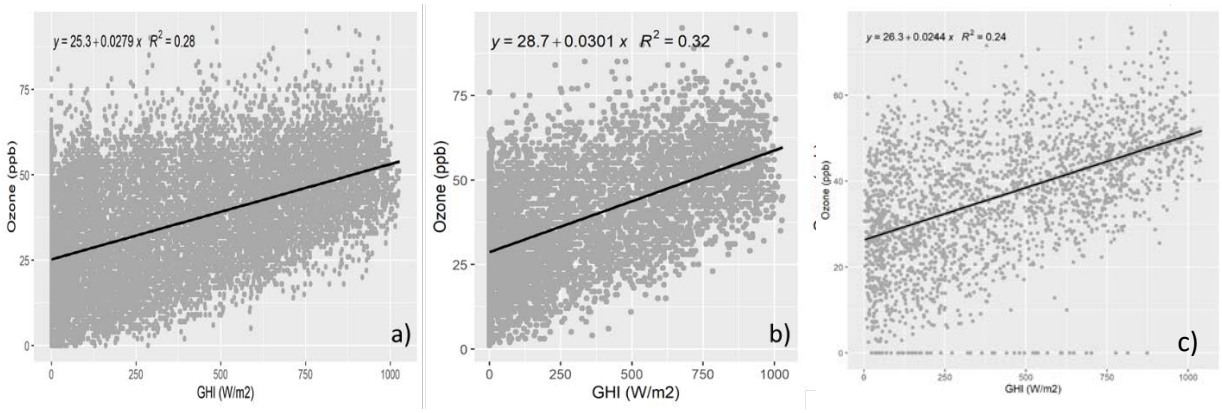

Figure 5: Positive correlation of O_3 and solar radiation during years a) 2013-2017 b) 2018-2019 c) 2020. The different grouped years have similar slopes.

Ozone and other Independent Variables

The objective of this study was to assess the effects of several meteorological variables on ground level ozone concentrations through linear regression and quantile analysis. Table 2 provides linear regression statistics for correlations between O_3 and several independent variables.

Table 2: Linear Regression statistics for several correlation studies. The dependent variable (y) is O_3 and the independent variable (x) is a meteorological variable.

Independent Variable (x)	**Linear Regression (2013-2017)**	**Linear Regression (2018-2019)**	**Linear Regression (2020)**	**R^2 (2013-2017; 2018-2019; 2020)**
Temperature (^OC)	y=1.64x-4.49	y=1.73x-4.54	y=1.7=13x+6.96	0.34; 0.38; 0.25

Relative Humidity (%)	y=-0.578x+67.3	y=-0.591x+73.6	y=-0.492x+65.1	0.38; 0.45; 0.43
Pressure (mb)	y=-0.398x+433	y=-0.430x+469	y=-0.551x+589	0.02; 0.02; 0.05
GHI (Wm^{-2})	y=0.0279x+25.3	y=0.0301x+28.7	y=0.0244x+26.3	0.28; 0.32; 0.24
Precipitation (inches; day before)	y=-1.83x+31.7	y=-2.34x+35.4	y=-2.34x+35.4	<0.01; <0.01; <0.01
Wind Speed (boundary layer)	y=1.12x+25	y=1.13x+27.9	y=1.10x+25.8	0.04; 0.04; 0.05
Wind Speed (500 mb)	y=-0.0361x+32.6	y=-0.162x+39.6	y=-0.051x+33.4	<0.01; 0.03; <0.01
Geopotential height (m)	y=0.00251x-108	y=0.00209x-87.2	y=0.000049x+29	0.02; 0.01; <0.01

Although low in correlation, ozone is inversely related to pressure and the prior day's precipitation. When looking at the upper atmosphere variables, ozone is inversely related to wind speed and positively correlated to the geopotential height.

Ozone and Wind Direction

Wind direction at ground-level and in the upper atmosphere, play an important role in the determination of ozone levels in the District. Here, we look at the wind direction's effect on the top 5% values of ozone during the years 2013-2017, 2018-2019 and 2020 (May 1-October 31) with violin plots (see Figure 6). Violin plots depict the distribution of numerical data using density curves. Surface-level winds out of the southwest contributed to the greatest median of ground-level ozone in 2020, while winds from the northeast and northwest at 500 mb and 850 mb contributed the greatest median ground-level ozone, respectively. Larger distributions of ozone were observed from surface-level winds out the south, southwest, and southeast. For years 2013-2019, surface-level winds from the south led to a higher median of ozone, and winds out of the southwest contributed to higher level ozone during the years 2018-2019. More information about the contribution of upper atmosphere wind direction is shown in Figure 6.

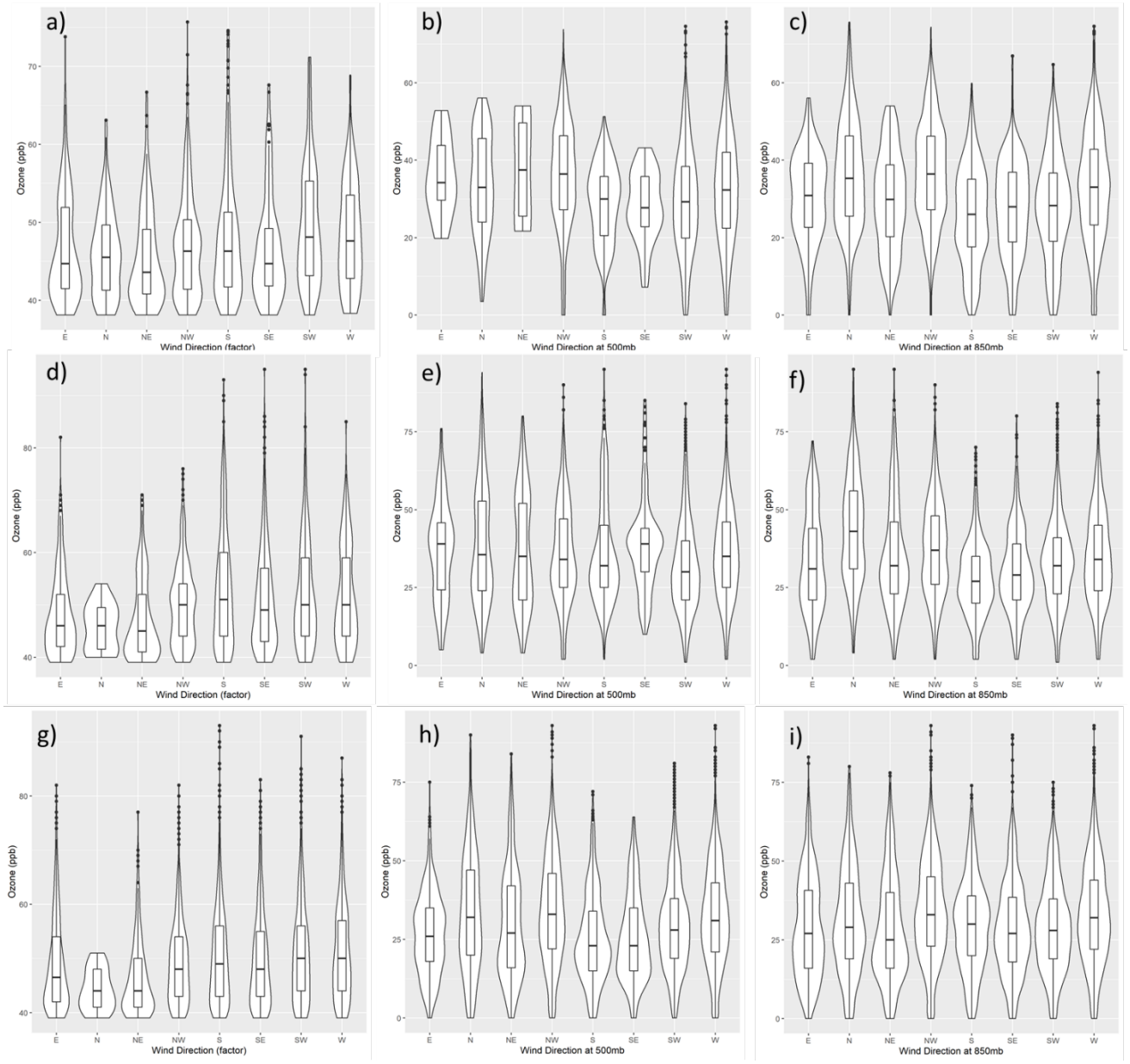

Figure 6: Violin plots depicting the effect of ground-level and upper-atmosphere wind direction on the surface-level ozone for the three different datasets: (a) 2013-2017 ground-level wind direction (b) 2013-2017 wind direction at 500 mb (c) 2013-17 wind direction at 850 mb (d) 2018-2019 ground-level wind direction (e) 2018-2019 wind direction at 500 mb (f) 2018-2019 wind direction at 850 mb (g) 2020 ground-level wind direction (h) 2020 wind direction at 500 mb and (i) 2020 wind direction at 850 mb.

Ozone's relationship with Day of the Week and Time of Day

Ground-level hourly ozone was monitored daily in the District. The ozone levels were compared for different days of the week and at various hours of the day. In 2020, the median ozone was greatest on Wednesday, with the largest distribution of data found on Tuesday, Wednesday and Thursday. Greatest ozone levels were observed during the mid-day hours (12 pm- 3pm local) as expected. Unlike 2020, the greatest median of ozone was observed during the weekend for years 2018-2019. However, the time of day trend for 2018-2019 matches year 2020. As observed with 2018-2019, the greatest ozone median occurred during the weekend for years 2013-2017. Peak ozone was also reached during the mid-day hours of 12 pm-3pm local time.

QR and OLS Compared to Observed Values

QR and OLS models were used to forecast ozone levels in the District. Figures 7a-h shows time series of predicted values (using QR and OLS) and the measured data for the ozone seasons of 2013-2020. Additional graphs comparing the coefficients of OLS and QR at different percentiles for all 55 regressors are provided in Supplemental Information (Figure S1). Generally, the models capture the peaks, but not always the magnitude. Table 3 shows the performance indexes of the three datasets using both models. It was observed that the QR model had the lowest magnitude for NMB during years 2014-2017. All years exhibited positive NMB values using QR. On the other hand, the OLS model underpredicted for every year except for 2020. The 2019 and 2020 NMB, NME and RMSE OLS value were lower in magnitude, when compared to QR during those two years. Thus, the OLS model predicted the District's ozone levels during the exceptional event, and during the year with the highest number of 90^{o}F days best (2019; 34 days). The RMSE measures the quality of the fit of the model, where a value of zero indicates a perfect fit. The average RMSE value for the QR model (2013-2020) was 3.10 while the average

RMSE value for OLS was 3.04. Overall, the OLS model was more efficient at forecasting ozone concentrations and proves to be beneficial for developing strategies to improve public health.

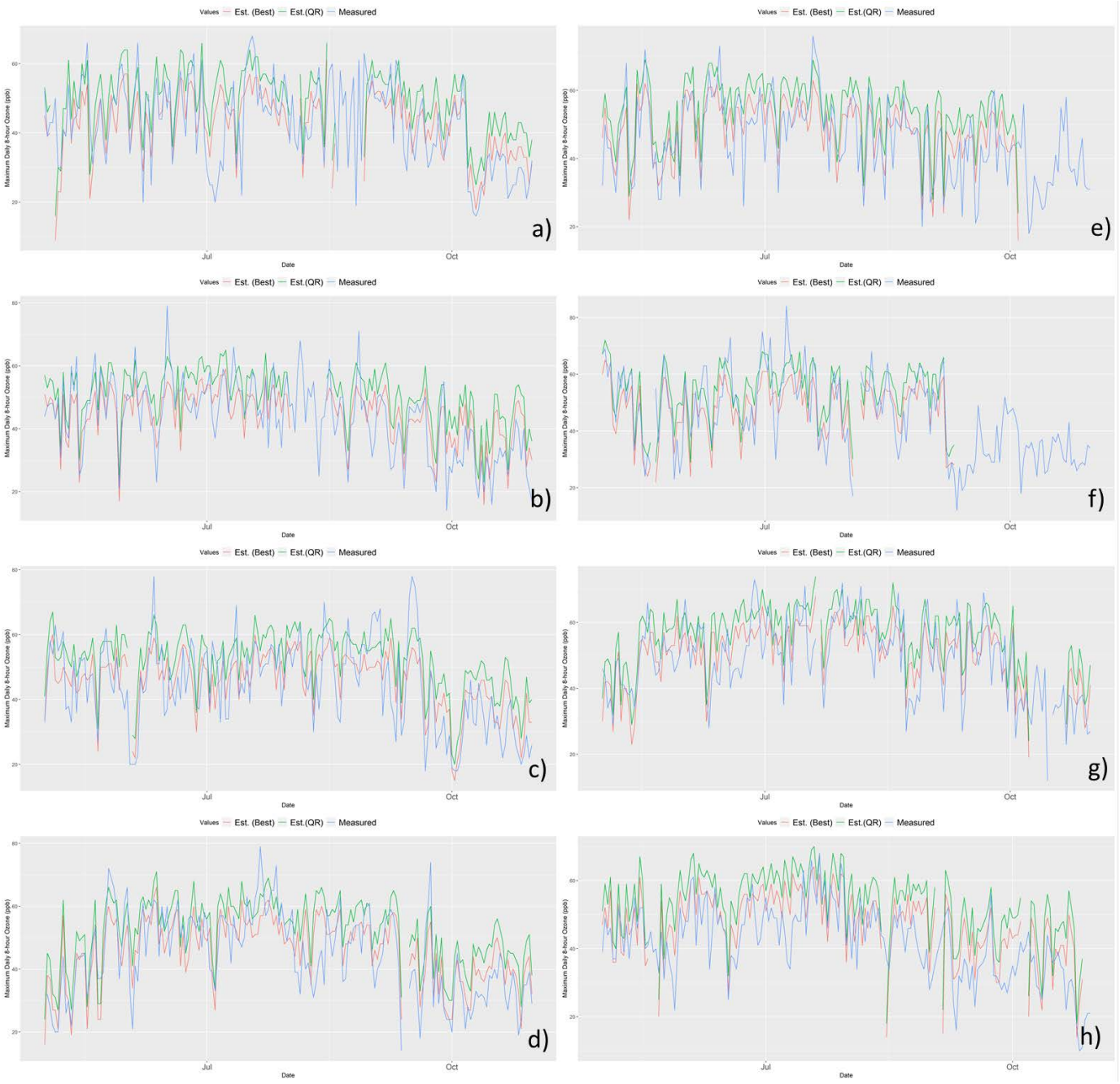

Figure 7: Time series of the maximum daily 8-hour ozone during the ozone seasons of (a) 2013 (b) 2014 (c) 2015 (d) 2016 (e) 2017 (f) 2018 (g) 2019 (h) 2020. Shown here are the measured (blue line) and the predicted values from the OLS (red line) and QR (green line) models.

Table 3: Performance indexes of the models (OLS and QR) achieved for years 2013-2020 where max daily 8-hour ozone was 60 ppb.

Year	**NMB**		**NME**		**RMSE**	
	OLS	**QR**	**OLS**	**QR**	**OLS**	**QR**
2013	-6.39	7.97	14.73	15.69	2.5	3.2195
2014	-14.33	0.89	18.69	13.12	6.037	0.3741
2015	-12.95	3.15	18.51	15.56	5.6147	1.3647
2016	-7.65	7.51	16.33	15.29	3.3217	3.2617
2017	-7.42	7.14	12.87	12.98	3.3601	3.2321
2018	-4.95	7.46	14.95	14.70	2.1894	3.3022
2019	-1.91	9.62	12.08	14.12	0.8359	4.2231
2020	0.82	12.77	10.58	14.53	0.375	5.8229

The performances of the models for the mean 8-hour daily ozone maximum and the 4th highest ozone maximum are shown in Figures 8a and 8b and numerical values are listed in Table S1 (Supplemental Information). The QR and OLS models over-predicted the 8-hour daily ozone maximum for every year in this study, except for 2013, where OLS slightly underpredicted by less than 1%. 2020 had the lowest measured value and the greatest difference in magnitude between both model predictions and the measured value. The estimated values of OLS and QR overpredicted by ~12% and ~26% for 2020, respectively. On the other hand, the 4th highest

ozone maximum OLS modelled values under-predicted for every year, ranging from ~2% to ~18%. The 4th highest maximum for 2013-2019 was 65+ ppb, whereas 2020 was the only year where the observed value measured below 65 ppb. Years 2013-2019 had a major influence from human activity while 2020 had a lesser human impact due to the pandemic. The QR model underpredicted for every year, except 2020. However, it was able to closely estimate the 4th highest maximum during year 2019 where there were the greatest number of extreme temperatures (90°F +). The QR modelled result was ~8% higher than the observed value during the 2020 pandemic. On the other hand, the OLS underpredicted to a smaller degree for 2020 (<2%). These changes in the OLS and QR modelled results for 2020 are likely attributed to the change in traffic patterns and anthropogenic emissions.

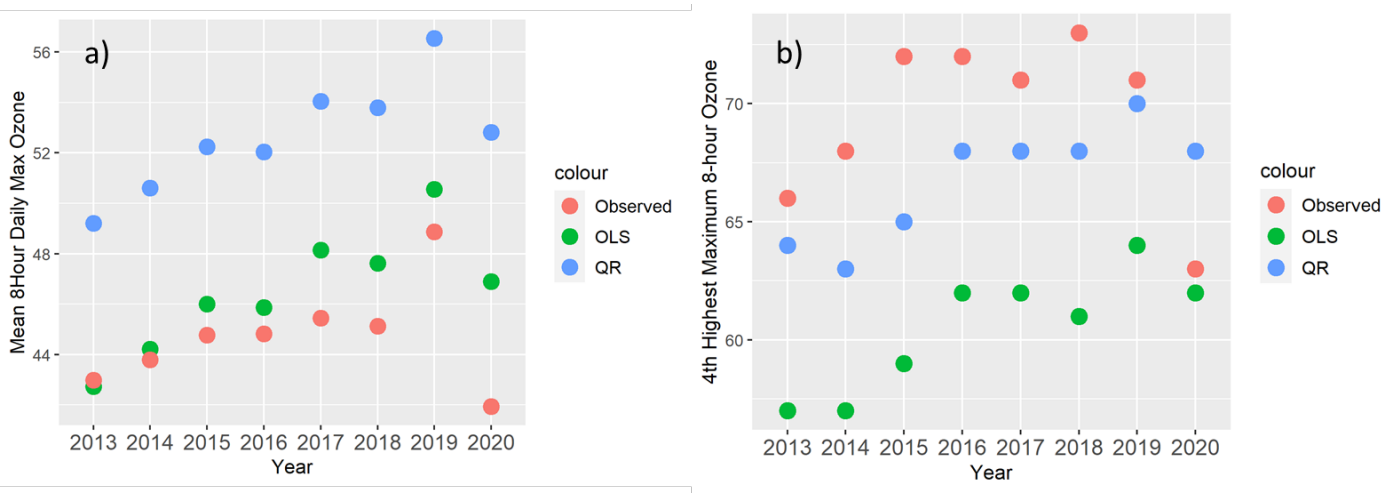

Figure 8: Plots of the mean (a) 8-hour daily ozone maximum and the (b) 4th highest ozone maximum during the ozone season for years 2013-2020.

Conclusions

In this study, the analysis of the impact of meteorological variables and ozone precursors on ozone concentrations for several years was performed. This paper characterizes the effect of

several parameters on ground-level ozone concentration in the District using OLS and QR models. The OLS model proved to be the most efficient model to predict ozone during the pandemic. Values of NMB, NME and RMSE were lower in magnitude for the OLS model during the pandemic year.

The year 2020 experienced a noticeable drop in ozone due to the Covid-19 shutdown. This event should be considered an exceptional event because it was unavoidable, believed to have occurred naturally and caused a disruption in traffic that is not likely to reoccur. Here, QR and OLS model results showed 2020 ozone season data was an outlier in comparison to years 2013-2019. For the mean daily 8-hour max, both models overestimated the ozone concentration for the years 2013-2019. However, the estimated value for both models were closer to the observed for 2020. On the other hand, the models' predictions were overestimated for the 4^{th} highest maximum of 8-hr ozone for the year 2020, and underpredicted for previous years. QR and OLS model results for 2020 sharply deviated from model results of the previous years and this is likely attributed to the difference in human activity. Future work should account for the association of traffic characteristics with ground-level ozone concentrations.

References

(1) Munir, S.; Chen, H.; Ropkins, K. Modelling the Impact of Road Traffic on Ground Level Ozone Concentration Using a Quantile Regression Approach. *Atmos. Environ.* **2012**, *60*, 283–291. https://doi.org/10.1016/j.atmosenv.2012.06.043.

(2) Vautard, R.; Beekmann, M.; Desplat, J.; Hodzic, A.; Morel, S. Air Quality in Europe during the Summer of 2003 as a Prototype of Air Quality in a Warmer Climate. *Comptes Rendus Geosci.* **2007**, *339* (11), 747–763. https://doi.org/10.1016/j.crte.2007.08.003.

(3) Jacob, D. J.; Winner, D. A. Effect of Climate Change on Air Quality. *Atmos. Environ.* **2009**, *43* (1), 51–63. https://doi.org/10.1016/j.atmosenv.2008.09.051.

(4) Dawson, J. P.; Adams, P. J.; Pandis, S. N. Sensitivity of Ozone to Summertime Climate in the Eastern USA: A Modeling Case Study. *Atmos. Environ.* **2007**, *41* (7), 1494–1511. https://doi.org/10.1016/j.atmosenv.2006.10.033.

(5) Camalier, L.; Cox, W.; Dolwick, P. The Effects of Meteorology on Ozone in Urban Areas and Their Use in Assessing Ozone Trends. *Atmos. Environ.* **2007**, *41* (33), 7127–7137. https://doi.org/10.1016/j.atmosenv.2007.04.061.

(6) Fix, M. J.; Cooley, D.; Hodzic, A.; Gilleland, E.; Russell, B. T.; Porter, W. C.; Pfister, G. G. Observed and Predicted Sensitivities of Extreme Surface Ozone to Meteorological Drivers in Three US Cities. *Atmos. Environ.* **2018**, *176*, 292–300. https://doi.org/10.1016/j.atmosenv.2017.12.036.

(7) Oyola, M. I.; Schneider, A.; Campbell, J.; Joseph, E. Meteorological Influences on Tropospheric Ozone over Suburban Washington, DC. *Aerosol Air Qual. Res.* **2018**, *18* (5), 1168–1182. https://doi.org/10.4209/aaqr.2017.12.0574.

(8) Munir, S.; Chen, H.; Ropkins, K. Characterising the Temporal Variations of Ground-Level Ozone and Its Relationship with Traffic-Related Air Pollutants in the United Kingdom: A Quantile Regression Approach. *Int. J. Sustain. Dev. Plan.* **2014**, *9* (1), 29–41. https://doi.org/10.2495/SDP-V9-N1-29-41.

(9) 2020 Ambient Air Quality Trends Report.Pdf.

(10) TSD-National-Emissions-Inventory-V6.3-USEPA-August-2016.Pdf.

(11) Chen, L.-W. A.; Chien, L.-C.; Li, Y.; Lin, G. Nonuniform Impacts of COVID-19 Lockdown on Air Quality over the United States. *Sci. Total Environ.* **2020**, *745*, 141105. https://doi.org/10.1016/j.scitotenv.2020.141105.

(12) Steinbrecht, W.; Kubistin, D.; Plass-Dülmer, C.; Davies, J.; Tarasick, D. W.; Gathen, P. von der; Deckelmann, H.; Jepsen, N.; Kivi, R.; Lyall, N.; Palm, M.; Notholt, J.; Kois, B.; Oelsner, P.; Allaart, M.; Piters, A.; Gill, M.; Malderen, R. V.; Delcloo, A. W.; Sussmann, R.; Mahieu, E.; Servais, C.; Romanens, G.; Stübi, R.; Ancellet, G.; Godin-Beekmann, S.; Yamanouchi, S.; Strong, K.; Johnson, B.; Cullis, P.; Petropavlovskikh, I.; Hannigan, J. W.; Hernandez, J.-L.; Rodriguez, A. D.; Nakano, T.; Chouza, F.; Leblanc, T.; Torres, C.; Garcia, O.; Röhling, A. N.; Schneider, M.; Blumenstock, T.; Tully, M.; Paton-Walsh, C.; Jones, N.; Querel, R.; Strahan, S.; Stauffer, R. M.; Thompson, A. M.; Inness, A.; Engelen, R.; Chang, K.-L.; Cooper, O. R. COVID-19 Crisis Reduces Free Tropospheric Ozone Across the Northern Hemisphere. *Geophys. Res. Lett.* **2021**, *48* (5), e2020GL091987. https://doi.org/10.1029/2020GL091987.

(13) Barré, J.; Petetin, H.; Colette, A.; Guevara, M.; Peuch, V.-H.; Rouil, L.; Engelen, R.; Inness, A.; Flemming, J.; Pérez García-Pando, C.; Bowdalo, D.; Meleux, F.; Geels, C.; Christensen, J. H.; Gauss, M.; Benedictow, A.; Tsyro, S.; Friese, E.; Struzewska, J.; Kaminski, J. W.; Douros, J.; Timmermans, R.; Robertson, L.; Adani, M.; Jorba, O.; Joly, M.; Kouznetsov, R. Estimating Lockdown-Induced European NO_2 Changes Using Satellite and Surface Observations

and Air Quality Models. *Atmospheric Chem. Phys.* **2021**, *21* (9), 7373–7394. https://doi.org/10.5194/acp-21-7373-2021.

(14) Guevara, M.; Jorba Casellas, O.; Soret, A.; Petetin, H.; Bowdalo, D.; Serradell Maronda, K.; Tena, C.; Gon, H. D. van der; Kuenen, J.; Peuch, V.-H.; Pérez García-Pando, C. Time-Resolved Emission Reductions for Atmospheric Chemistry Modelling in Europe during the COVID-19 Lockdowns. *Atmospheric Chem. Phys.* **2021**, *21*, 773–779. https://doi.org/10.5194/acp-21-773-2021.

(15) Goldberg, D. L.; Anenberg, S. C.; Griffin, D.; McLinden, C. A.; Lu, Z.; Streets, D. G. Disentangling the Impact of the COVID-19 Lockdowns on Urban NO2 From Natural Variability. *Geophys. Res. Lett.* **2020**, *47* (17), e2020GL089269. https://doi.org/10.1029/2020GL089269.

(16) Pishue, B. *2020 Global Traffic Scorecard*; INRIX, 2021; p 23.

(17) Sousa, S. I. V.; Pires, J. C. M.; Martins, F. G.; Pereira, M. C.; Alvim-Ferraz, M. C. M. Potentialities of Quantile Regression to Predict Ozone Concentrations. *Environmetrics* **2009**, *20* (2), 147–158. https://doi.org/10.1002/env.916.

(18) Wyoming Weather Web http://weather.uwyo.edu/upperair/ (accessed 2021 -06 -17).

(19) Guillory, A. ERA5 https://www.ecmwf.int/en/forecasts/datasets/reanalysis-datasets/era5 (accessed 2021 -06 -17).

(20) Koenker, R.; Bassett, G. Regression Quantiles. *Econometrica* **1978**, *46* (1), 33–50. https://doi.org/10.2307/1913643.

(21) Baur, D.; Saisana, M.; Schulze, N. Modelling the Effects of Meteorological Variables on Ozone Concentration—a Quantile Regression Approach. *Atmos. Environ.* **2004**, *38* (28), 4689–4699. https://doi.org/10.1016/j.atmosenv.2004.05.028.

(22) Dueñas, C.; Fernández, M. C.; Cañete, S.; Carretero, J.; Liger, E. Assessment of Ozone Variations and Meteorological Effects in an Urban Area in the Mediterranean Coast. *Sci. Total Environ.* **2002**, *299* (1–3), 97–113. https://doi.org/10.1016/S0048-9697(02)00251-6.

(23) Elminir, H. K. Dependence of Urban Air Pollutants on Meteorology. *Sci. Total Environ.* **2005**, *350* (1), 225–237. https://doi.org/10.1016/j.scitotenv.2005.01.043.

(24) Tu, J.; Xia, Z.-G.; Wang, H.; Li, W. Temporal Variations in Surface Ozone and Its Precursors and Meteorological Effects at an Urban Site in China. *Atmospheric Res.* **2007**, *85* (3), 310–337. https://doi.org/10.1016/j.atmosres.2007.02.003.

(25) Shan, W.; Yin, Y.; Zhang, J.; Ji, X.; Deng, X. Surface Ozone and Meteorological Condition in a Single Year at an Urban Site in Central–Eastern China. *Environ. Monit. Assess.* **2009**, *151* (1), 127–141. https://doi.org/10.1007/s10661-008-0255-0.

(26) Shan, W.; Yin, Y.; Zhang, J.; Ding, Y. Observational Study of Surface Ozone at an Urban Site in East China. *Atmospheric Res.* **2008**, *89* (3), 252–261. https://doi.org/10.1016/j.atmosres.2008.02.014.

(27) Kavassalis, S. C.; Murphy, J. G. Understanding Ozone-Meteorology Correlations: A Role for Dry Deposition. *Geophys. Res. Lett.* **2017**, *44* (6), 2922–2931. https://doi.org/10.1002/2016GL071791.

(28) Dabdub, D.; DeHaan, L. L.; Seinfeld, J. H. Analysis of Ozone in the San Joaquin Valley of California. *Atmos. Environ.* **1999**, *33* (16), 2501–2514. https://doi.org/10.1016/S1352-2310(98)00256-8.

(29) Rodríguez, S.; Guerra, J.-C. Monitoring of Ozone in a Marine Environment in Tenerife (Canary Islands). *Atmos. Environ.* **2001**, *35* (10), 1829–1841. https://doi.org/10.1016/S1352-2310(00)00550-1.

(30) Xu, D.; Yap, D.; Taylor, P. A. Meteorologically Adjusted Ground Level Ozone Trends in Ontario. *Atmos. Environ.* **1996**, *30* (7), 1117–1124. https://doi.org/10.1016/1352-2310(95)00331-2.

(31) Roberts–Semple, D.; Song, F.; Gao, Y. Seasonal Characteristics of Ambient Nitrogen Oxides and Ground–Level Ozone in Metropolitan Northeastern New Jersey. *Atmospheric Pollut. Res.* **2012**, *3* (2), 247–257. https://doi.org/10.5094/APR.2012.027.